REPORT DOCUMENTATION PAGE

Form Approved
OMB No. 0704-01-0188

1. REPORT DATE *(DD-MM-YYYY)*
08-04-2005

2. REPORT TYPE
REPRINT

3. DATES COVERED *(From - To)*

4. TITLE AND SUBTITLE
Nascap-2k Spacecraft Charging Code Overview

5a. CONTRACT NUMBER

5b. GRANT NUMBER

5c. PROGRAM ELEMENT NUMBER
61102F

5d. PROJECT NUMBER
5021

5e. TASK NUMBER
RS

5f. WORK UNIT NUMBER
A1

6. AUTHORS
M.J Mandell*, V.A. Davis*, D.L. Cooke, A.T. Wheelock, and C.J. Roth**

7. PERFORMING ORGANIZATION NAME(S) AND ADDRESS(ES)
Air Force Research Laboratory /VSBXT
29 Randolph Road
Hanscom AFB, MA 01731-3010

8. PERFORMING ORGANIZATION REPORT NUMBER
AFRL-RV-HA-TR-2007-1141

9. SPONSORING/MONITORING AGENCY NAME(S) AND ADDRESS(ES)

10. SPONSOR/MONITOR'S ACRONYM(S)
AFRL/VSBXT

11. SPONSOR/MONITOR'S REPORT NUMBER(S)

12. DISTRIBUTION/AVAILABILITY STATEMENT
Approved for Public Release; distribution unlimited.

13. SUPPLEMENTARY NOTES
Reprinted from Proceedings, 9th Spacecraft Charging Technology Conference, Tsukuba, Japan, 4-8 April 2005. .
* Science Applications International Corp., San Diego, CA 92121 **Radex, Inc., Lexington, MA 02421

14. ABSTRACT
Nascap-2k is a modern spacecraft charging code, replacing the older codes NASCAP/GEO, NASCAP/LEO, POLAR, and DynaPAC. The code builds on the physical principles, mathematical algorithms, and user experience developed over three decades of spacecraft charging research. Capabilities include surface charging in geosynchronous and interplanetary orbits, sheath and wake structure and current collection in low-Earth orbits, and auroral charging. External potential structure and particle trajectories are computed using a finite element method on a nested grid structure and may be visualized within the *Nascap-2k* interface. Space charge can be treated either analytically, self-consistently with particle trajectories, or by importing plume densities from an external code such as *EPIC* (Electric Propulsion Interactions Code). Particle-in-cell capabilities are available to study dynamic plasma effects. Auxiliary programs to *Nascap-2k* include *Object Toolkit* (for developing spacecraft surface models) and *GridTool* (for constructing nested grid structures around spacecraft models). The capabilities of the code are illustrated by way of four examples: charging of a geostationary satellite, self-consistent potentials for a negative probe in a LEO spacecraft wake, potentials associated with thruster plumes, and PIC simulations of plasma effects on a VLF (about 1 to 20 kHz) antenna.

15. SUBJECT TERMS
Spacecraft charging Plasma simulation, Nascap-2k

16. SECURITY CLASSIFICATION OF: a. REPORT	b. ABSTRACT	c. THIS PAGE	17. LIMITATION OF ABSTRACT	18. NUMBER OF PAGES
UNCL	UNCL	UNCL	UNL	24

19a. NAME OF RESPONSIBLE PERSON
Adrian Wheelock

19B. TELEPHONE NUMBER *(Include area code)*

NASCAP-2K SPACECRAFT CHARGING CODE OVERVIEW

M. J. Mandell, (858) 826-1622, Myron.J.Mandell@saic.com
V.A. Davis, (858) 826-1608, Victoria.A.Davis@saic.com
Science Applications International Corporation
10260 Campus Point Dr., M.S. A1A, San Diego, CA, 92121 (FAX: 858-826-6584)

D. L. Cooke, A.T. Wheelock
Air Force Research Laboratory, Space Vehicles Directorate
Hanscom Air Force Base, MA 01731 (FAX: 781-377-2491)

C. J. Roth
Radex Inc.
131 Hartwell Ave. Lexington MA, 02421-3126

Abstract

Nascap-2k is a modern spacecraft charging code, replacing the older codes NASCAP/GEO, NASCAP/LEO, POLAR, and DynaPAC. The code builds on the physical principles, mathematical algorithms, and user experience developed over three decades of spacecraft charging research.

Capabilities include surface charging in geosynchronous and interplanetary orbits, sheath and wake structure and current collection in low-Earth orbits, and auroral charging. External potential structure and particle trajectories are computed using a finite element method on a nested grid structure and may be visualized within the *Nascap-2k* interface. Space charge can be treated either analytically, self-consistently with particle trajectories, or consistent with imported plume densities. Particle-in-cell (PIC) capabilities are available to study dynamic plasma effects.

Auxiliary programs to *Nascap-2k* include *Object Toolkit* (for developing spacecraft surface models) and *GridTool* (for constructing nested grid structures around spacecraft models).

The capabilities of the code are illustrated by way of four examples: charging of a geostationary satellite, self-consistent potentials for a negative probe in a LEO spacecraft wake, potentials associated with thruster plumes, and PIC calculations of plasma effects on a VLF (about 1 to 20 kHz) antenna.

Introduction

Designers of spacecraft for government, commercial, and research purposes require advanced modeling capabilities to guide the design of satellites that can survive and operate properly in the natural environment. Computer modeling of flight experiments (including SCATHA, the SPEAR[1,2] series, and CHAWS[3]) demonstrated excellent ability to predict both steady-state and dynamic interactions between high-voltage spacecraft and the ambient plasma. This ability was extended to inherently dynamic problems involving three-dimensional space charge sheath formation, current flow in the quasi-neutral presheath, breakdown phenomena, plasma kinetics, ionization processes, and the effect of unsteady processes on spacecraft charging.

NASCAP/GEO[4,5,6] (NASA Charging Analyzer Program for GEosynchronous Orbit) was the standard tool for the computation of spacecraft charging in tenuous plasmas for more than two decades. Since then, the fully three-dimensional computer codes NASCAP/LEO[7,8] (NASA Charging Analyzer Program for Low-Earth Orbit), POLAR[9] (Potentials Of Large objects in the Auroral Region), and DynaPAC[10] (Dynamic Plasma Analysis Code) were developed to address various other spacecraft-plasma interactions issues. *Nascap-2k*[11] builds on the capabilities of these older codes, giving the spacecraft designer much-improved modeling capabilities by taking advantage of a greater understanding of the pertinent phenomena, employing more advanced algorithms, and implementing a state-of-the-art user interface, including three-dimensional post-processing graphics. *Nascap-2k* is being developed by Science Applications International Corporation (SAIC) as part of a program sponsored jointly by the Air Force Research

Laboratory at Hanscom AFB and by NASA's Space Environments and Effects (SEE) Program at Marshall Space Flight Center. The current release is Version 3.1.

Nascap-2k is an interactive toolkit for studying plasma interactions with realistic spacecraft in three dimensions. As it incorporates physics developed for all the previous codes, it can solve problems appropriate to both tenuous (*e.g.*, GEO orbit or interplanetary missions) and dense (*e.g.*, LEO orbit) plasma environments. *Nascap-2k* is targeted to spacecraft design engineers, spacecraft charging researchers, and aerospace engineering students. The graphical user interface is designed to help less experienced users easily solve moderately complex plasma interactions problems. Figure 1 shows several views of the *Nascap-2k* interface, including the main problem setup page, the *GridTool* interface, and views of particle trajectories and space and surface potentials.

The core capabilities of *Nascap-2k* include:

1. Define spacecraft surfaces and geometry and the structure of the computational space surrounding the spacecraft;
2. Solve for time-dependent potentials on spacecraft surfaces;
3. Solve the electrostatic potential about the object, with flexible boundary conditions on the object and with space-charge computed either fully by particles, fully analytically, or in a hybrid manner;
4. Generate, track, and otherwise process electrons and ions, represented as macroparticles in the computational space; and
5. View surface potentials, space potentials, particle trajectories, and time-dependent potentials and currents.

To accomplish these capabilities, *Nascap-2k* consists of:

1. The *Nascap-2k* graphical user interface (Figure 1), a user-friendly environment for definition of problem parameters, strategizing and running calculations, and visualizing results;
2. *Object ToolKit* (OTk), an interactive program for the definition of spacecraft surfaces;
3. *GridTool*, an interactive program to create arbitrarily subdivided grids in the space surrounding a spacecraft model;
4. The modules that comprised the *DynaPAC* code as the major computational engine. These have been converted to DLLs (dynamic link libraries) to run seamlessly within *Nascap-2k*;
5. A new analysis module implementing the Boundary Element Method[12] (BEM) for calculating surface charging in Geosynchronous Earth Orbit (GEO), in the Solar Wind, or in other tenuous plasma environments.

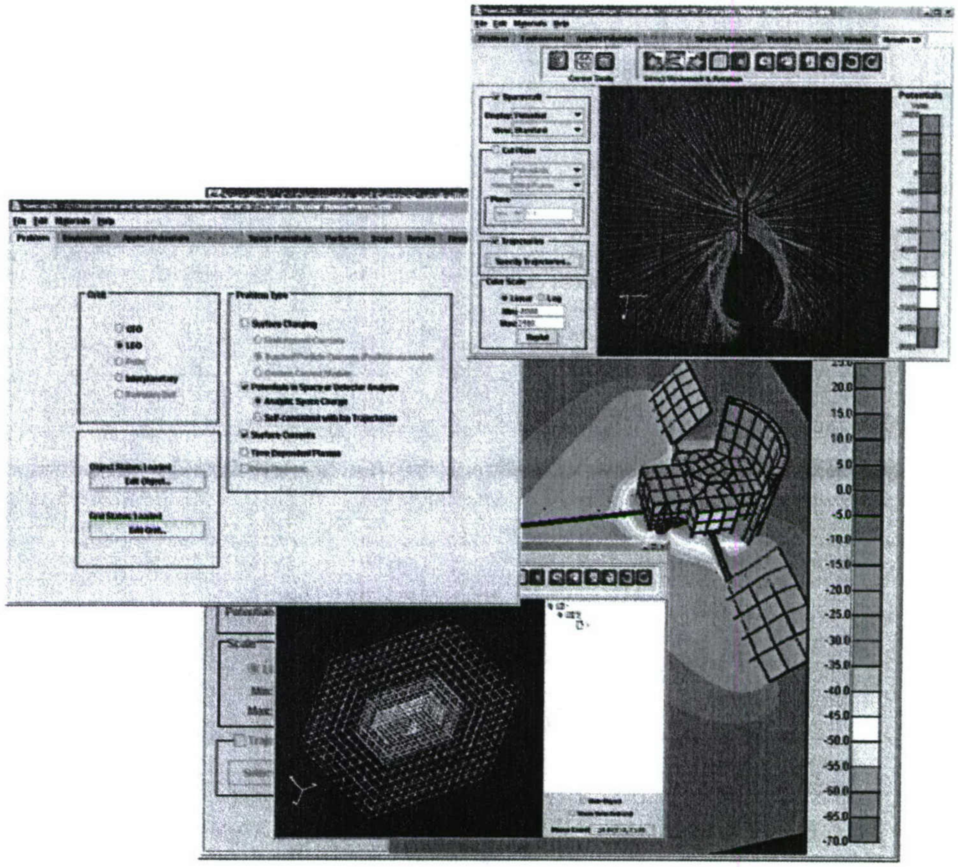

Figure 1. Views of the *Nascap-2k* tabbed user interface, including main problem setup (center left), particle trajectories (upper right), surface and space potentials (center right), and *GridTool* interface (bottom center).

Nascap-2k uses a high-order finite element representation for the electrostatic potential that assures that electric fields are strictly continuous throughout space. The electrostatic potential solver (originally developed for *DynaPAC*[13]) uses a conjugate gradient technique to solve for the potentials and fields on the spacecraft surface and through the surrounding space. Several analytic and numerical space charge density models are available, including Laplacian, Linear, Non-linear, Frozen Ions, Full Trajectory Ions, Hybrid PIC (appropriate to the several microsecond timescale response to a negative pulse), and Full PIC.

Particle tracking is used to study sheath currents, to study detector response, to generate steady-state charge densities, or to generate space charge evolution for dynamic calculations. *Nascap-2k* generates macroparticles (each of which represents a collection of particles) either at a "sheath boundary", the problem boundary, or throughout all space. Alternatively, particles can be initialized with a user-generated file. Particles are tracked for a specified amount of time, with the timestep automatically subdivided at each step of each particle to maintain accuracy. The current to each surface element of the spacecraft is recorded for further processing.

The **Results 3D** tab of the *Nascap-2k* user interface is used to generate graphical output illustrating such quantities as object surface potentials, space potentials, particle positions, or particle trajectories. Using Java3D capabilities, these figures can be rotated, panned, zoomed, or measured. Contour levels and other plotting attributes are modified through the user interface. The **Results** tab is used to view time histories and obtain numerical values for potentials and surface currents.

The modular structure of *Nascap-2k* is illustrated in Figure 2. Surface charging is done in the new **Charge Surfaces** module. Space potentials and particle trajectories are calculated with DLLs built from the *DynaPAC* modules[10]. The suite of codes is written in Java (user interface), C++ and Fortran (science), and C (utility routines) and is maintained on the Win32 platform. (*Nascap-2k* has also been ported to Linux.)

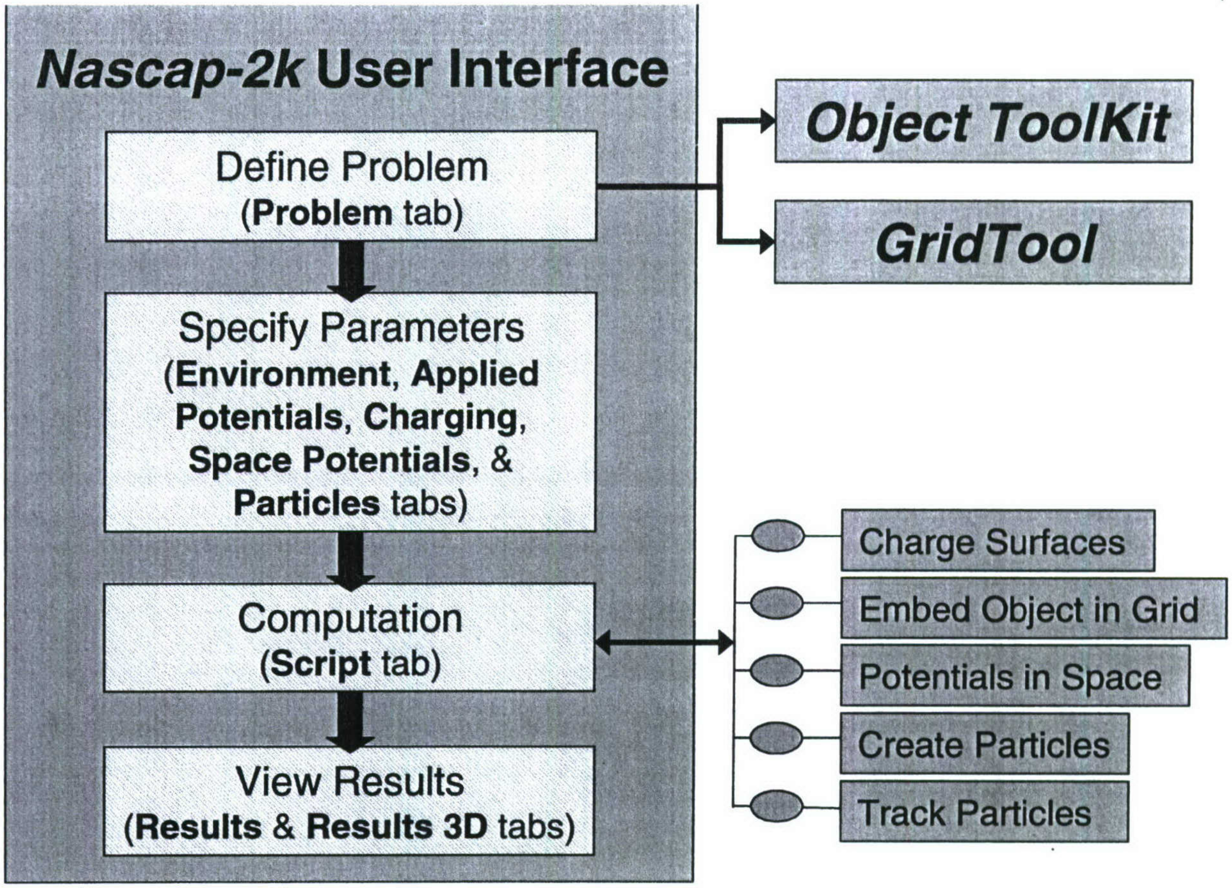

Figure 2. *Nascap-2k* Module Diagram.

Spacecraft Models and Object Toolkit

A Nascap-2k application usually begins by building a geometrical spacecraft model with *Object Toolkit*. Objects are built using the five native components shown in Figure 3, together with components imported from standard finite element preprocessing software and components previously defined and saved using *Object Toolkit*. Direct mesh editing capabilities are available to create subdivision and to build components with complex shapes. **Figure 4** and **Figure 5** show examples of spacecraft defined using *Object Toolkit*.

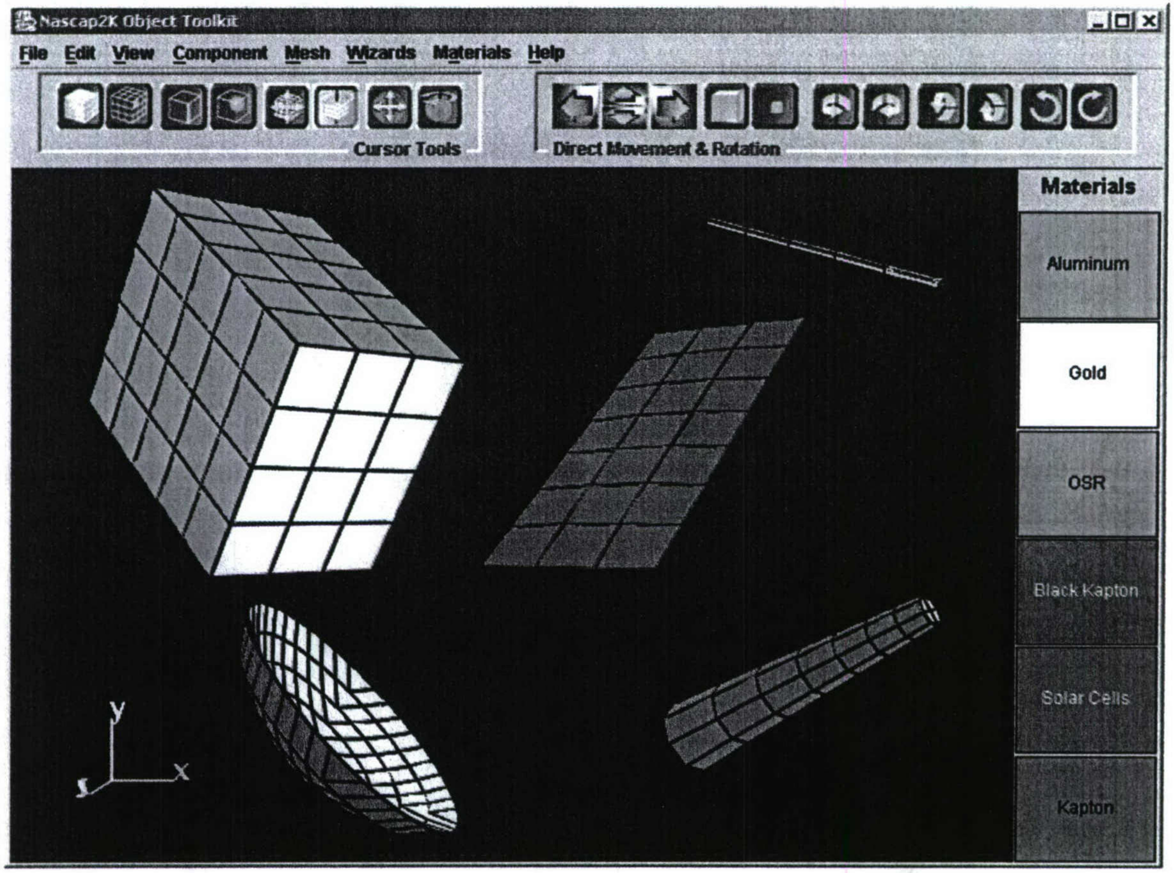

Figure 3. Native components (clockwise from upper left: Box, Boom, Panel, Cylinder, Dish) available within *Object Toolkit* for defining spacecraft models.

Each surface element of a spacecraft model has attributes of "Conductor Number" and "Material Name." The conductor number attribute is used to represent electrical circuitry coupling the spacecraft surfaces, such as biasing of surfaces or capacitive/resistive coupling. With each material name is associated a list of properties including thickness, bulk and surface conductivity, and photoemission and secondary electron emission coefficients. Material properties can be edited in both *Object Toolkit* and the main *Nascap-2k* interfaces. In addition, advanced features such as grounding tabs can be placed on the spacecraft model.

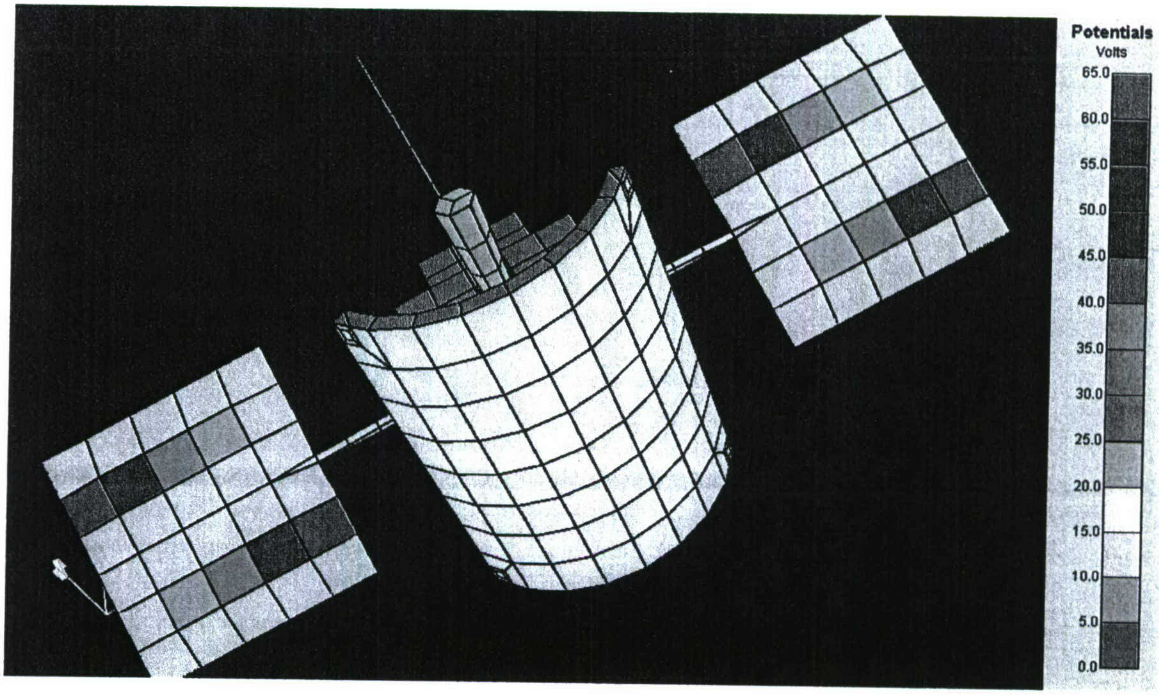

Figure 4. *Nascap-2k* model of the MESSENGER spacecraft, showing biased solar array surfaces.

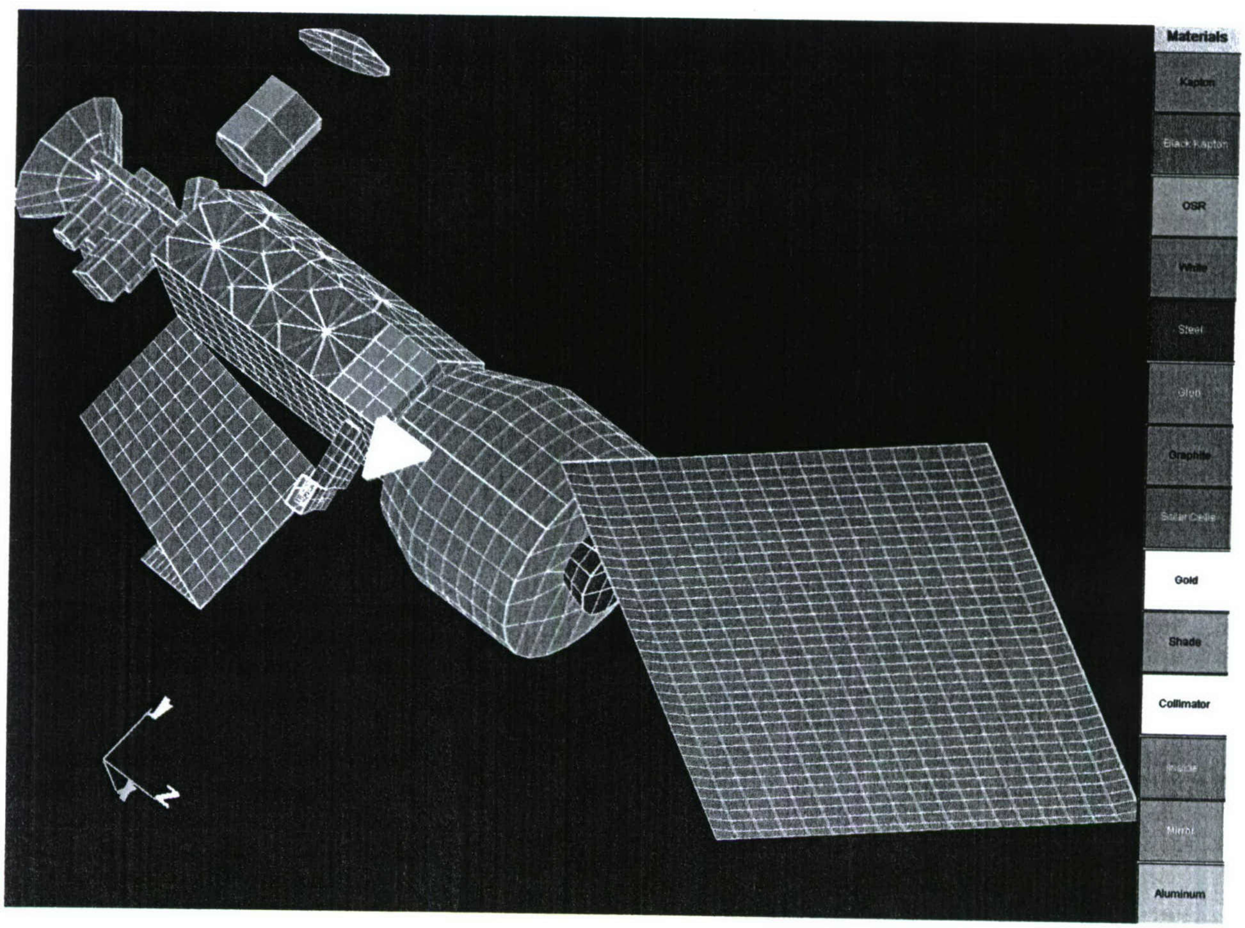

Figure 5. DMSP spacecraft model constructed in *Object Toolkit*.

Example 1: Geosynchronous Orbit Charging

The earliest and most common application for this family of codes is to study charging of spacecraft in geostationary orbit. *Nascap-2k* is designed to make this type of analysis particularly easy.

A simple *Object Toolkit*-built model of a geosynchronous spacecraft is shown in Figure 6. Apart from the solar arrays, the spacecraft is covered with low-secondary-emission insulators, except for some patches of high-secondary-emission OSRs on the side of the box. Since *Nascap-2k* can calculate surface potentials and electric fields using the Boundary Element Method (BEM), a simple charging calculation does not require a spatial grid. Addition of a grid would enable the calculation and display of space potentials and particle trajectories.

Nascap-2k contains a selection of predefined Maxwellian, Double Maxwellian, and auroral plasma environments, which are readily modified to create custom environments. For this example we use the "NASA Worst Case" environment[14] consisting of Maxwellian electrons and H+ ions, shown in Table 1. Other aspects of the environment include the magnetic field (here set to zero), the sun direction (shining directly on the solar panels) and the sun intensity (set to solar intensity at 1 AU).

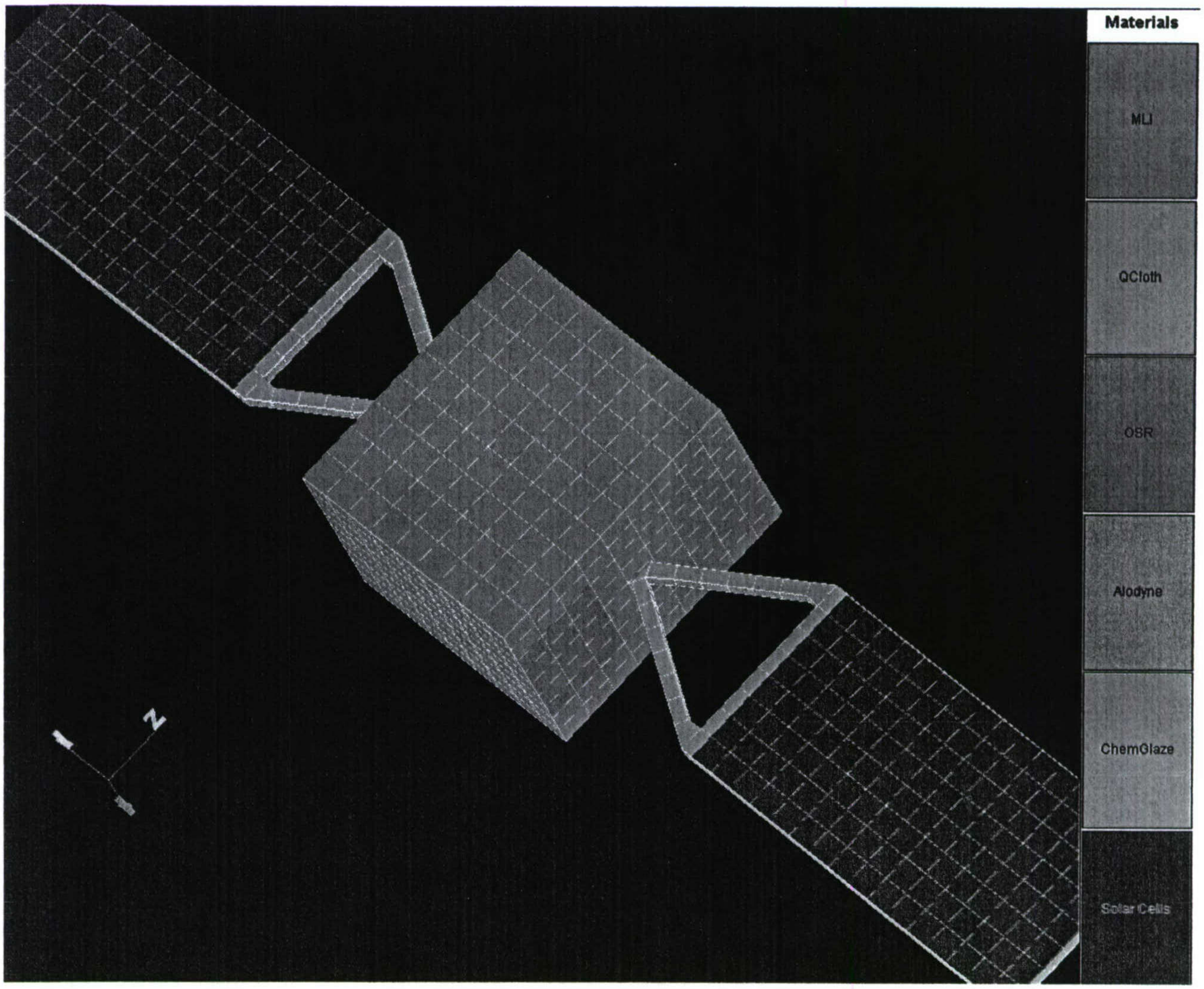

Figure 6. Simple geosynchronous spacecraft used for example. The central box is about 2 m in each dimension, and each solar panel is 1.5 m wide and 3 m long.

Table 1. Parameters of "NASA Worst Case" environment.[14]

	H^+	e^-
Density	0.236×10^6 m^{-3}	1.12×10^6 m^{-3}
Temperature	29.5 keV	12 keV

Users have control of the parameters governing the calculations and the sequence of operations (script) that compose the simulation. In this case, the timestepping parameters were edited to produce more, shorter time steps than the default, and the automatically generated script was used without modification. Exposing the script provides a great deal of flexibility in running problems with *Nascap-2k*. Customized scripts can be built and edited both within the **Script** tab and externally using a text editor or specialized XML editor. During the calculation "monitors" display the progress of the simulation.

Calculation results are post-processed and displayed on the **Results3D** tab (Figure 7) and on the **Results** tab. Figure 7 shows that, after five minutes of charging, most of the dark surface material charges to about 10 kV negative, with the emissive OSR surfaces about 8 kV negative. The least negative surface elements, at about 7 kV negative, are at the center of the sunlit side of the central box and toward the outboard end of the solar arrays. As shown in Figure 7, we can select individual surface elements to obtain detailed information about them. In a gridded calculation, this tab can define and display contour planes of external potential and particle trajectories superposed on the surface plot.

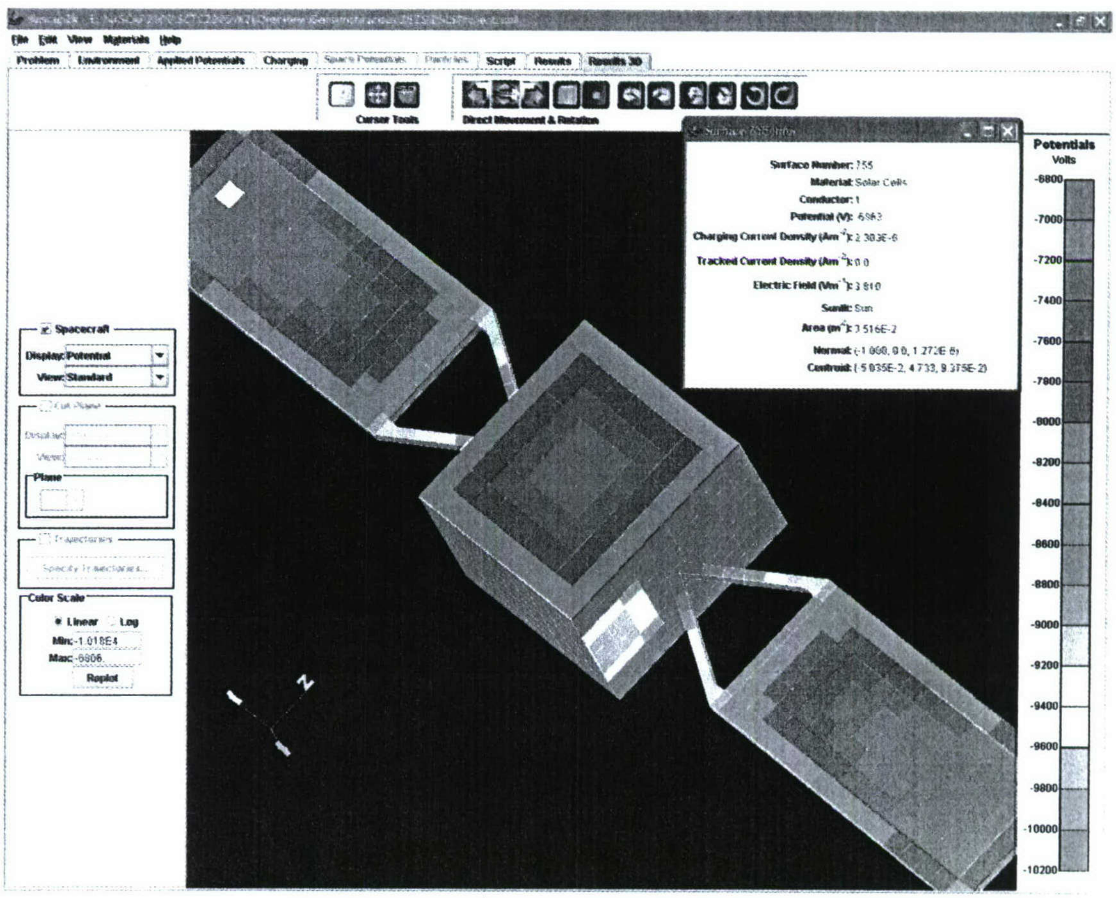

Figure 7. Results3D tab showing surface potentials at end of calculation, and detailed information for a selected surface element.

The **Results** tab is used to display detailed numerical and time-dependent information, such as potentials, electric fields, or currents, for groups of surface elements, individual surface elements, or conductor entities. This information is available both as line plots and as text that can be pasted into a spreadsheet for further processing. Figure 8 shows time-dependent potentials of various surfaces plotted using the Microsoft Excel spreadsheet program.

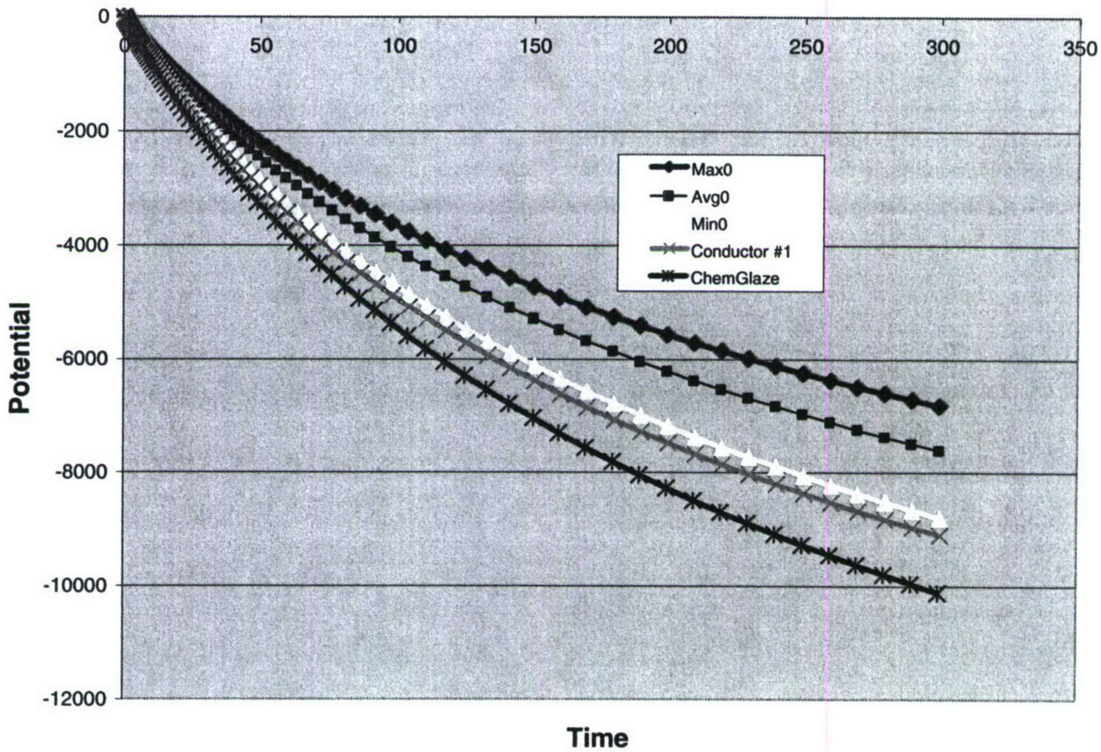

Figure 8. Time-dependent potentials of solar array surfaces (upper three curves), spacecraft ground (second from bottom) and dark, insulating Chemglaze (bottom) plotted after importing results into Microsoft Excel.

Example 2: Self-Consistent Potentials in a Wake

To study ion collection by a high voltage object in a spacecraft wake, the CHAWS[3] (Charging Hazards and Wake Studies) experiment was flown aboard the WSF (Wake Shield Facility) on STS-60 (February 1994) and STS-69 (September 1995). Originally simulated using the *DynaPAC* code, we use this problem as the primary example of a self-consistent (between potentials and trajectories) calculation in *Nascap-2k.*

Figure 9 shows the Object Toolkit model of the WSF with CHAWS. The CHAWS probe is the off-center well-resolved rod seen toward the left of the figure, which shows the wake side of the WSF. Negative biases of up to 2 kV were applied to the probe, which was instrumented to measure both the total current and the distribution of current over the surface.

Since we need to calculate both space potentials and particle trajectories, a grid structure is built in the space surrounding the model. The *GridTool* representation of the grid structure is shown in Figure 10. The grid is designed to provide high resolution both in the neighborhood of the probe and in the region of plasma flow that is perturbed by the applied potential.

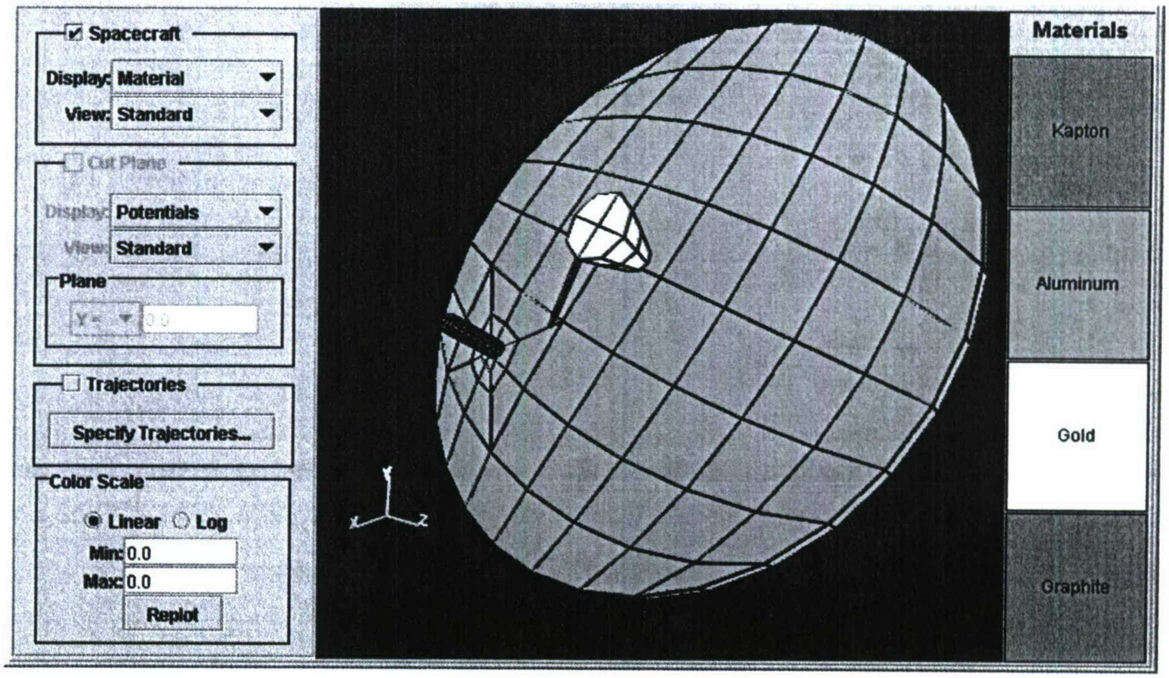

Figure 9. Geometric model of the WSF wake side, showing the CHAWS probe (well-resolved cylinder at left). The WSF is 3.66 m in diameter, and the probe is 46 cm long and located 51 cm from the edge of the WSF.

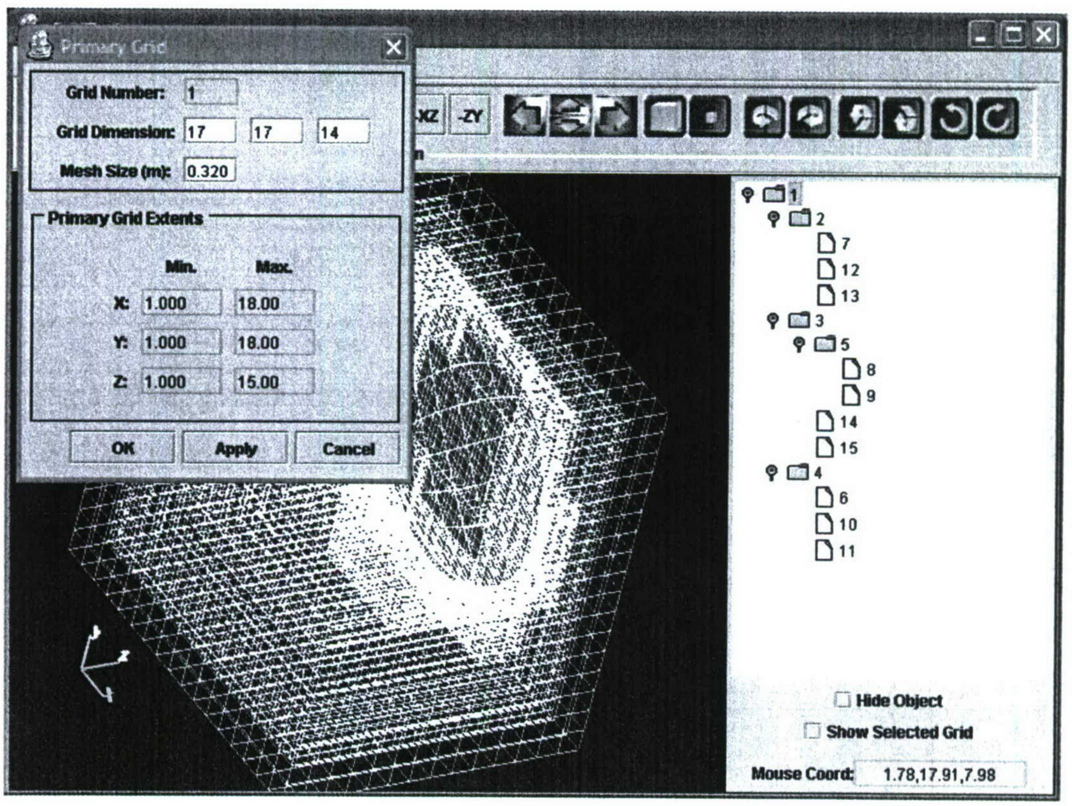

Figure 10. *GridTool* view of grid structure used for the CHAWS problem. The right pane details the grid and subgrid structure. The grid is over 5 m across with coarsest resolution of 32 cm, and fine resolution of 4 cm in the neighborhood of the CHAWS probe and the edge of the WSF nearest the probe.

The environment specification for this problem includes not only the plasma density and temperature (1×10^{11} m^{-3} and 0.1 eV), but also the spacecraft velocity (7800 m s^{-1}) and the ion species (90% O^+ and 10% H^+), which together determine the ram ion energy. The script for this calculation, which is generated automatically by *Nascap-2k*, directs the code to generate and track particles in the existing potentials, and then recalculate the potentials using space charge derived from the ion trajectories. (The electron density is assumed to be barometric.) The sequence repeats to approach a self-consistent solution. The script also refers to input files (which are generated automatically and can also be user-edited) to the *Nascap-2k* modules and to the output files from those modules.

Figure 11 shows a subset of O^+ ion trajectories for this problem. Ions are generated at the problem boundary with a thermal spread about the ram direction and are tracked until they strike the object or leave the problem space. Ion space charge is accumulated in the grid at each tracking step, and the current corresponding to ions reaching the CHAWS probe is recorded. It is noteworthy that no ions strike the side of the probe nearest the edge of the WSF, but rather ions either strike the tip of the probe or else miss the tip and are attracted back to the side of the probe facing the center of the WSF.

Finally, Figure 12 displays the self-consistent potentials about the CHAWS probe behind the WSF. Note that the potential field of the probe extends nearly 0.4 m into the ram flow in the vicinity of the near edge of the WSF, and the resulting electric fields cause the deflection of ions from this region into the wake where they may be collected by the probe, as seen in Figure 11. The grounded rear surface of the WSF, the WSF instrumentation, and the space charge contribution of ions deflected into the wake all play a role in screening the potential of the high-voltage CHAWS probe. As a result, the potential within the wake downstream of the probe falls off considerably faster than would be the case if the probe were in a cylindrical vacuum region.

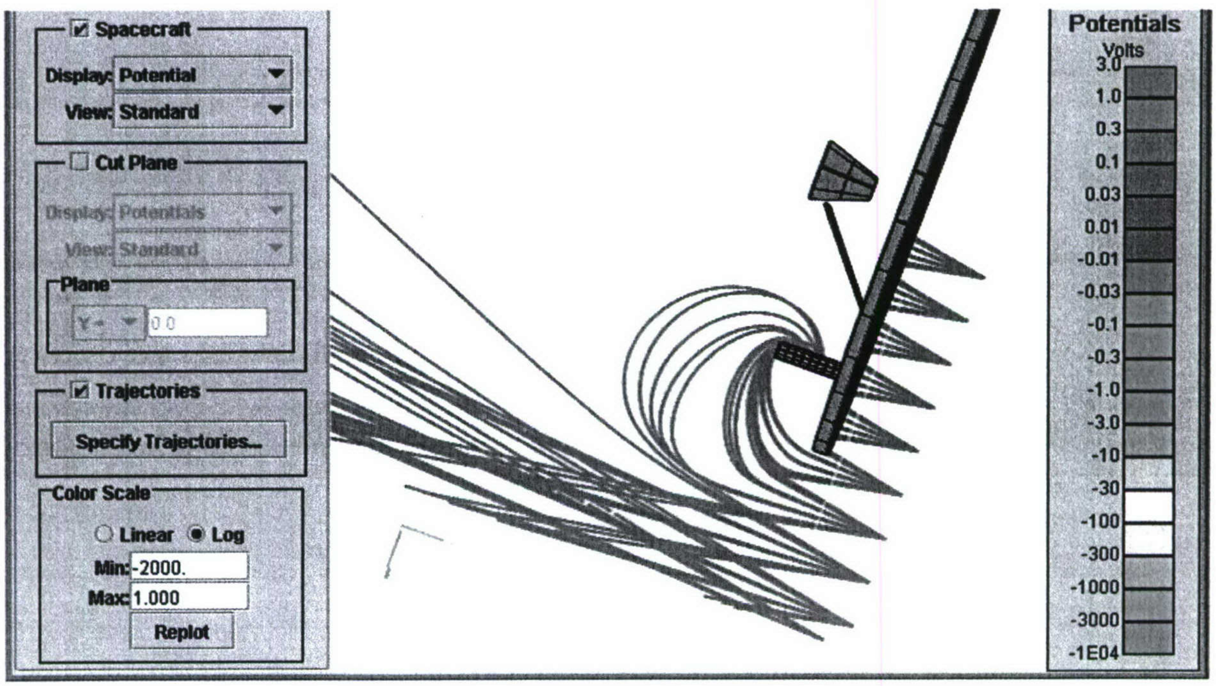

Figure 11. Trajectories of ram particles, including thermal spread, for CHAWS problem.

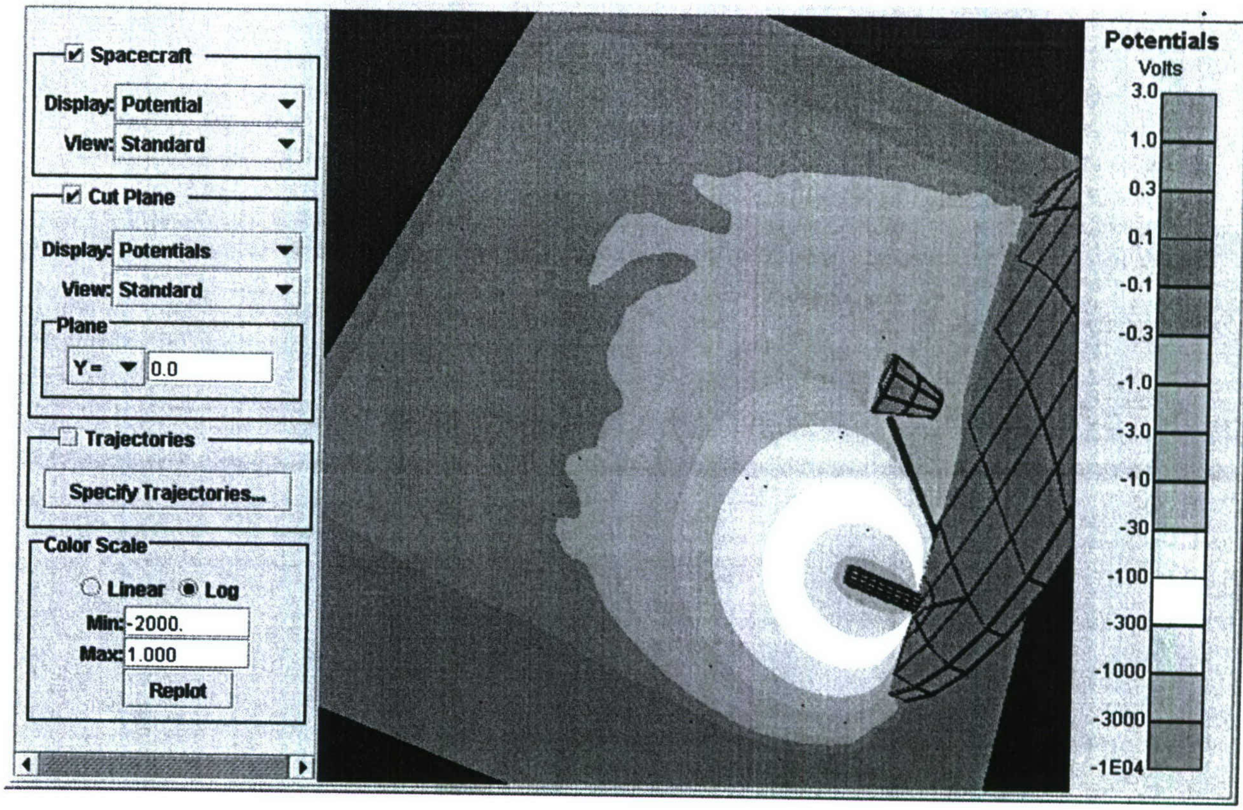

Figure 12. Self-consistent potentials about the CHAWS probe in the wake of the WSF.

Comparison of these calculations with the actual CHAWS measurements is discussed in Reference 3. For negative probe biases exceeding 100 volts the probe sheath penetrates the ram flow and the measured total current to the probe (as well as its distribution over the probe) is in good agreement with calculations after secondary electron emission (due to impact of energetic ions) is taken into account. However, the calculations predict a sharp drop in current when the bias drops below 100 volts. No such threshold is observed. We interpret this to mean that there is more plasma in the wake than expected, with ionospheric hydrogen, spacecraft thrusters, and outgassing being likely contributors to this wake plasma.

Example 3: Potentials in Electrostatic Thruster Plumes

A recent enhancement made to *Nascap-2k* is the inclusion of ion densities from plasma sources (such as thruster plumes) in the computation of potentials in space. One reason for needing potentials due to plasma sources is the computation of contaminant trajectories. We plan to extend this capability to study, among other phenomena, the influence of spacecraft surfaces on engine plumes and interactions between plumes.[16]

Nascap-2k's plume capabilities are intended to complement those of the *EPIC* (Electric Propulsion Interactions Code) computer code[15] which, like *Nascap-2k*, has been developed by SAIC for NASA's SEE program. *EPIC* is a fast-running code that models plumes, places plumes on spacecraft, displays plume densities in space, and calculates plume fluxes to spacecraft surfaces and resultant surface effects (*e.g.*, sputtering). It is easy to modify parameters in *EPIC*, as well as to account for orbital configuration changes (*e.g.*, rotation of solar arrays). However, *EPIC* does not calculate potentials in space, and thus cannot account for the effects of surface potentials and surface sheaths, interactions between plumes, or self-consistent flow of charge exchange ions around obstacles, all of which are intended subjects for study with *Nascap-2k*.

For this example the ion density due to plasma sources is imported into *Nascap-2k* from *EPIC*. The import is done via SOAP (an XML-based interprocess communication scheme formerly known as "Simple Object Access Protocol"). (Since this paper was originally presented we have added the capabilities to import a plume directly into *Nascap-2k*, to specify the locations and directions of multiple instances of the plume, and to generate and track charge exchange ions within *Nascap-2k* to achieve a self-consistent solution.[16]) *Nascap-2k* then solves a nonlinear Poisson equation for space potentials using the surface potentials as boundary conditions. As was done in the CHAWS example presented above, the charge density consists of a known ion density plus a barometric electron density:

$$\frac{\rho}{\varepsilon_0} = \frac{\rho_{ion}}{\varepsilon_0}\left(1 - \exp\left((\phi - \phi_b)/\theta\right)\right)$$

$$\phi_b = \theta \ln\left(\frac{\rho_{ion}}{en}\right)$$

where θ and n are the plume electron temperature and reference density respectively, ρ is the total charge density to be used in Poisson's equation, and ρ_{ion} is the known ion density, in this case imported from *EPIC*.

We treat a configuration that might characterize a geosynchronous spacecraft during North-South station-keeping. On the same spacecraft used above for the geostationary charging example, we affix two NSTAR[17] thrusters pointing NorthWest and NorthEast. (A thruster as large as NSTAR is unlikely to be used for this purpose, but we selected it because we had a good model for its plume.) Figure 13 shows the spacecraft and plasma densities as displayed in *EPIC*.

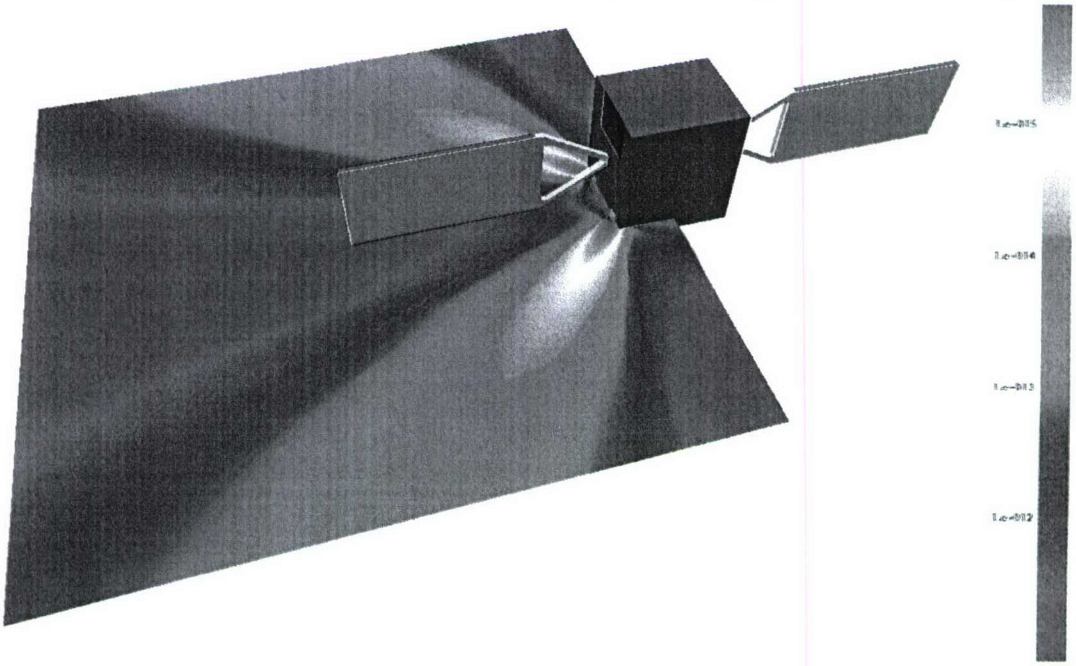

Figure 13. Plasma density displayed in *EPIC* for two NSTAR thrusters, as described in text.

For a reference density we chose a value of 1×10^{12} m^{-3}, which is the density of charge exchange ions just outside the main beam. This density is also used as the minimum ion density. Choosing the minimum ion density equal to the reference density has the effect of setting regions void of plume ions to zero potential. The beam electron temperature was taken as 1 eV. We set the average potential on the solar arrays to be +20 V, and the potential of all other surfaces to be -2 V. Figure 14 shows the resulting potentials in space, calculated by *Nascap-2k*. The contour plane of Figure 14 is chosen to contain the thrusters and the densest part of the plume. The positive potentials of the thruster plumes are clearly seen, and the sheath around the negative spacecraft body extends further on into the low density plasma on the side opposite the thrusters than it does into the denser plasma near the thrusters, illustrating treatment of interactions between surface potentials and the plume plasma. (The sheath near the 20 V solar array surfaces is not seen in the figure because the arrays do not intersect the contour plane.)

The plume capability is shown here at an early stage. This capability has been extended to include self-consistent generation and tracking of charge exchange ions, and is currently being used to analyze plume interactions, charge exchange ion density and flow, and surface impingement in multiple thruster tests[16] conducted at NASA Glenn Research Center during December 2005. Presentation of results is expected in Summer 2006.[18]

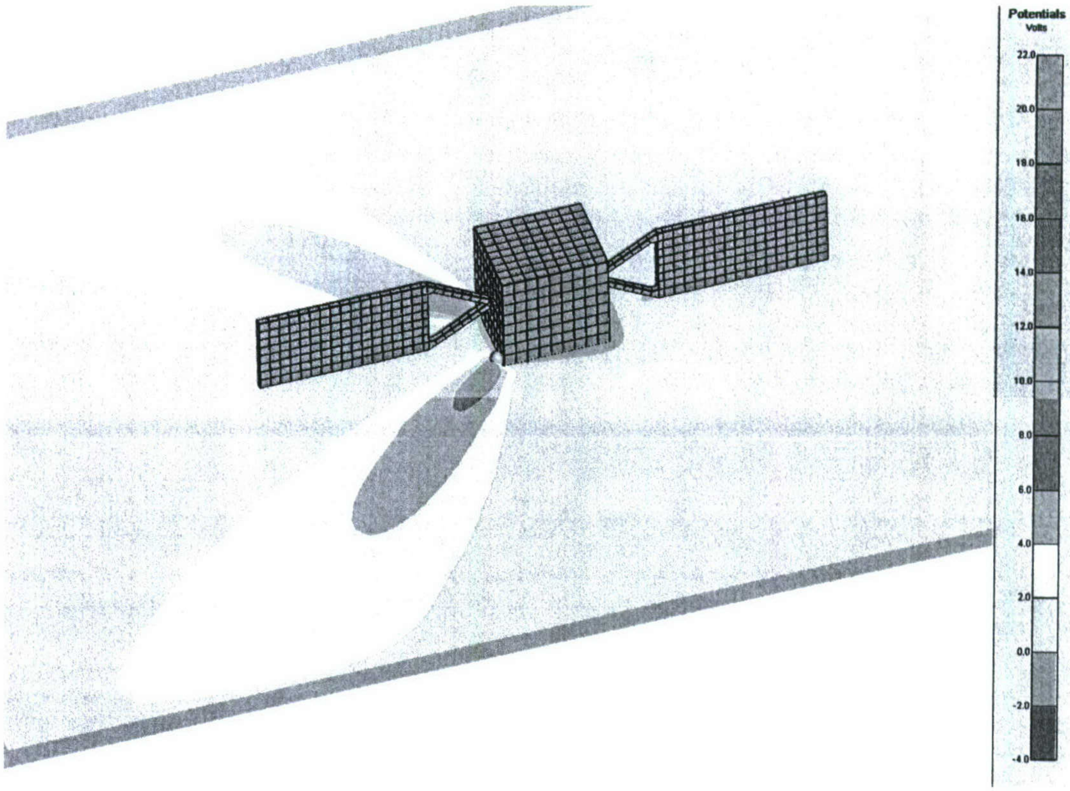

Figure 14. *Nascap-2k* display of space and surface potentials in the presence of the thruster plumes shown in **Figure 13**. Other parameters as described in the text.

Example 4. Plasma Effects on a VLF Antenna

There is current interest in VLF (about 1 to 20 kHz) antennas in the upper ionosphere because plasma waves with such frequencies are thought to interact with MeV radiation belt electrons. Such an antenna would be a rod several inches in diameter and many meters long and, due to the ease of electron collection by positive objects, would be nearly always at negative potential relative to the ambient ionosphere. Because the frequencies of interest are comparable to the ion plasma frequency, the sheath structure will be at some intermediate state between the "ion matrix" or "frozen ion" limit (which assumes the ions are stationary and contribute ambient ion density to the space charge) and the equilibrium space charge limit (in which the ions assume a steady-state space charge limited distribution of charge and current). Thus, calculation of the sheath structure and of the ion collection by the antenna requires dynamic (PIC) treatment, at least for the ions. Using *Nascap-2k* we can perform all four simulations of interest: (1) equilibrium space charge sheath; (2) "frozen ion" sheath; (3) dynamic PIC ions with fluid (Boltzmann or barometric) electrons (Hybrid PIC); (4) dynamic PIC ions and electrons (Full PIC).

Here we present highlights of calculations of types (3) and (4) as listed above. Table 2 lists the parameters for the two calculations. The Full PIC calculation, because of its short simulated time, focuses on electron dynamics, whereas the Hybrid PIC calculation illustrates ion dynamics. Also, to facilitate the calculation, the Full PIC simulation was done at higher frequency and higher plasma density (to obtain a smaller sheath).

Full PIC Calculation (Electron Dynamics)

Prior to performing the PIC calculation in *Nascap-2k*, we performed a one-dimensional (cylindrical) simulation of the same problem of sudden application of -100 volts to a 5 cm radius cylindrical antenna (as shown in the "PIC" column of **Table 2**). The results are shown in Figure 15. The sheath radius (dark line in Figure 15) is easily identified in these calculations as the boundary of the region from which electrons are excluded. Due to the high frequency content of the square wave, strong electron plasma oscillations are excited, and are manifested by oscillations of the sheath location, initially between radii of 30 cm and 10 cm. When the sheath is at its outermost position there is an excess of ions within the sheath, leading to the appearance of positive potentials (magenta line in Figure 15) as high as 70 volts just inside the sheath location (yellow line in Figure 15).when the sheath is at its maximum radius. When the sheath is at its innermost position there is an excess of electrons within the sheath, so that the potentials are everywhere negative, and the location of the maximum potential (yellow line in Figure 15) jumps to the computational boundary. We undertook the relatively modest task to reproduce in *Nascap-2k* the same simulation from initiation to the first maximum in sheath radius.

Table 2. Contrasting parameters for the PIC and Hybrid PIC simulations.

Parameter	**PIC**	**Hybrid-PIC**
Frequency	100 kHz	2, 6, 20 kHz
Plasma Density	3×10^{11} m^{-3}	1×10^{10} m^{-3}
Plasma Frequency (electron)	4.92 MHz	898 kHz
Plasma Frequency (Oxygen)	28.5 kHz	5.2 kHz
Peak applied potential	-100 V	-100 V
Waveform	Square wave	Sine Wave
Sheath radius	34 cm	80 cm
Timestep	2.5 ns	1/50f
Time Simulated	0.140 μs	2/f
Antenna Length	4 m	10 m
Antenna Radius	0.05 m	0.1 m
Initial No. of Electrons (Ions)	350,000	966,000

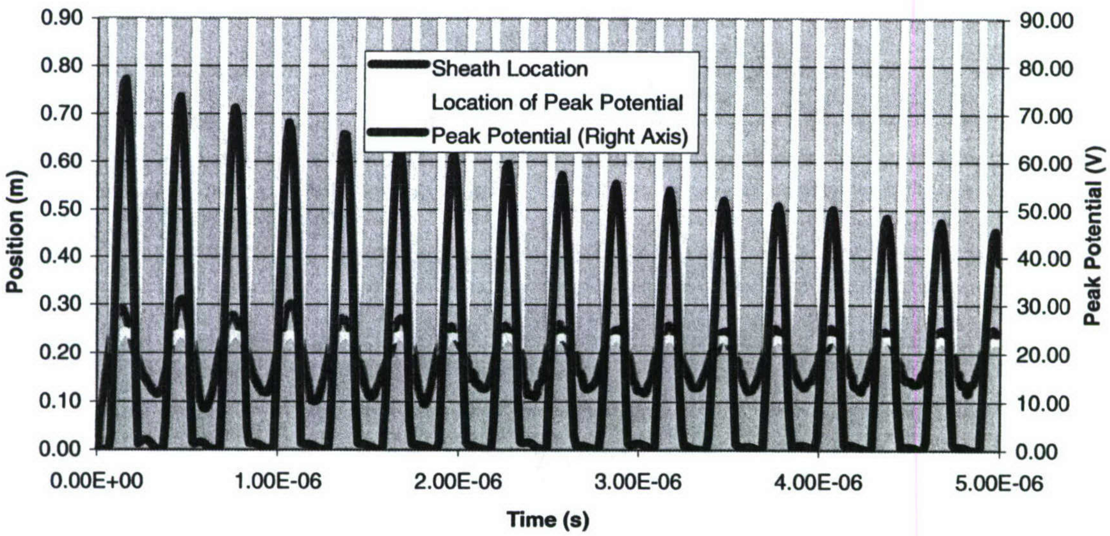

Figure 15. Sheath behavior for square-wave excitation calculated using one-dimensional full PIC cylindrical code. See problem parameters in "PIC" column of **Table 2**, and explanation in text.

Figure 16 shows the Nascap-2k antenna model and grid, with fine zoning in the neighborhood of the negative antenna element. Electron and ion macroparticles were created throughout the grid, as shown in Figure 17. After the negative potential was applied, electrons moved radially outward (Figure 18), leaving ions behind to form the observed positive potential. Figure 19 shows a plane of electron macroparticles superposed on the potentials along the antenna at the time of maximum sheath radius.

Finally, Figure 20 shows a comparison of the *Nascap-2k* results with those obtained using the one-dimensional cylindrical code. The sheath radius calculated by *Nascap-2k* is slightly larger due to the square cross-section antenna's being effectively larger than the cylindrical antenna simulated in the one-dimensional code. The time of maximum sheath radius and the magnitude of the maximum observed positive potential agree very well.

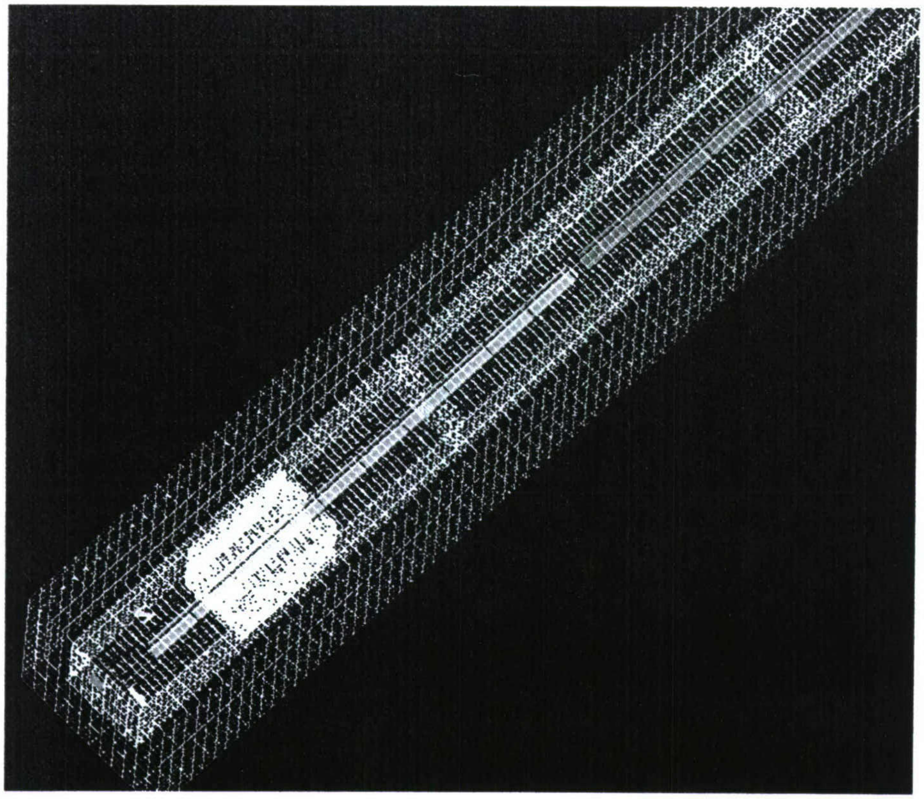

Figure 16. *Nascap-2k* antenna model, showing antenna and gridding. Each arm of the antenna is 4 m long, and has a 10 cm square cross-section. The computational mesh is 1.32 m square and 9.24 m long.

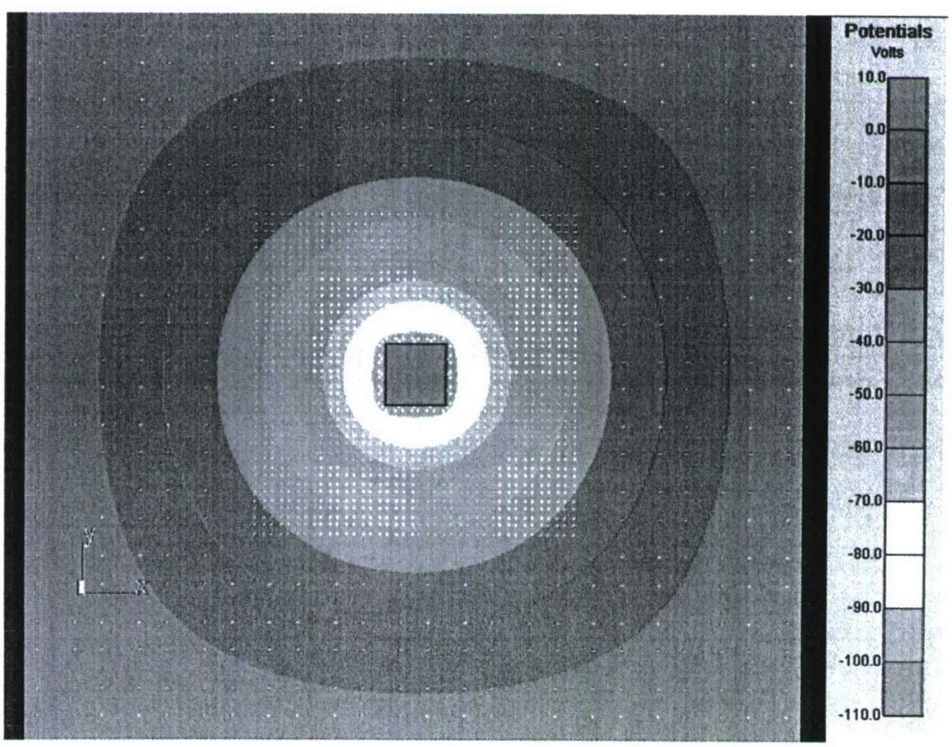

Figure 17. Planar view of initial potentials and particle positions.

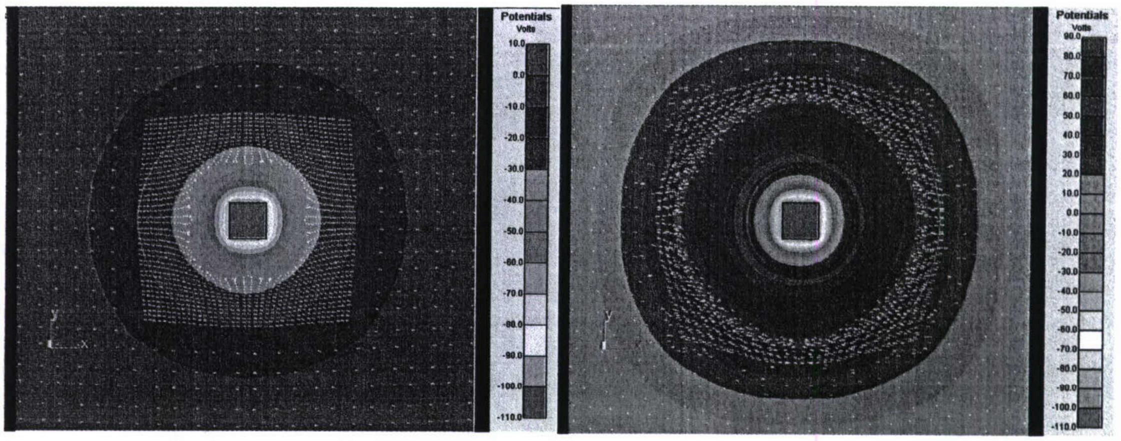

Figure 18. Blowups of electron macro-particles and potentials. Left: sheath radius of about 18 cm after 50 ns. Right: at time of maximum positive potential (137 ns).

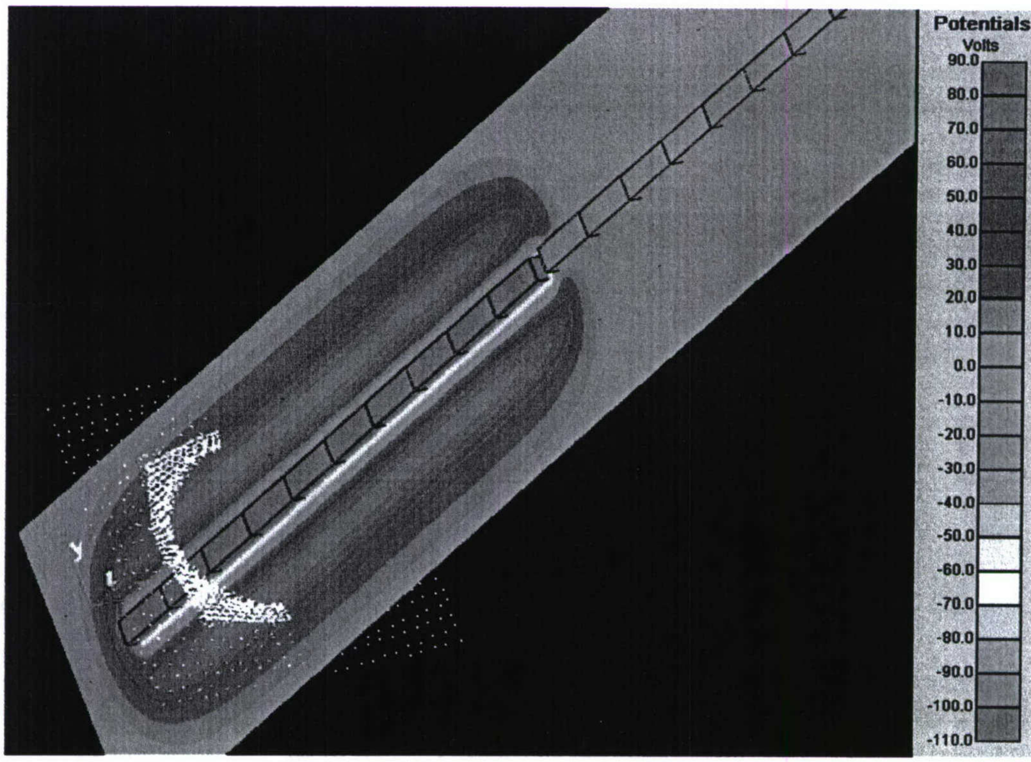

Figure 19. View of the final configuration (at 137.5 ns), showing a plane of electron macroparticles and potentials in a plane containing the antenna.

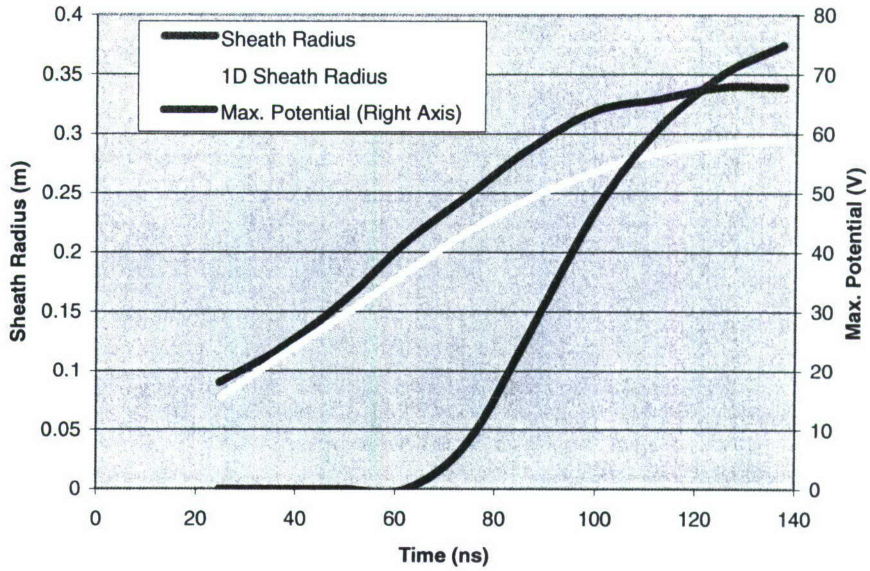

Figure 20. *Nascap-2k* results for sheath radius (dark curve) and maximum potential (magenta curve, right scale) compared with one-dimensional sheath radius results (yellow curve).

Hybrid PIC Calculation (Ion Dynamics)

To perform a calculation for parameters more nearly resembling the frequency, waveform, and plasma density of interest for VLF experiments, we eschewed following the electron dynamics and adopted the hybrid-PIC method, in which the electrons are assumed to always be in thermal equilibrium. The Hybrid PIC technique is appropriate for low frequency problems for which electrons behave as an equilibrium fluid, but ions must be treated as a kinetic gas using the PIC method. In this case, we used the simplest electron fluid, the Boltzmann equilibrium, and only the O^+ ions were tracked. The objective of the calculation is to obtain the magnitude and waveform for plasma current incident on the antenna.

Parameters for the PIC and hybrid-PIC calculations are contrasted in Table 2. Note that while the hybrid-PIC method allows the timestep to be much longer, the longer time to be simulated (with each timestep requiring a particle push and a nonlinear potential solution) and the larger sheath volume conspire to make both calculations of comparable difficulty. In addition, it can be shown that thermal effects are likely to be important as the sheath becomes large. Thus, the calculation was first performed with zero-temperature ions, and then with each initially stationary ion macro-particle replaced by a set of four macro-particles diverging at thermal speed in the plane normal to the antenna as a preliminary model of a thermal distribution. Only the results for thermal distribution are shown here, as they give a much smoother current waveform, probably due to having a larger number of lower-weight macroparticles.

Prudence dictates that the antenna center tap be DC-isolated from the spacecraft ground (which therefore remains near plasma ground), and simple calculations show that the positive arm of the antenna cannot go more than a few volts positive. Accordingly, the spacecraft and the positive portion of the antenna are maintained at plasma potential, while each antenna arm is biased with a negative half-cycle of applied voltage, followed by an equal period of near-zero potential. The potentials are solved at each time step.

A snapshot of the 2 kHz, zero temperature calculation is shown in Figure 21. The figure shows the potentials in a cut plane midway through the negative end of the antenna, and ion macroparticles flowing toward the antenna. Although only a representative subset of the ion macro-particles is shown, the figure still illustrates that *Nascap-2k* can perform this calculation with a relatively low number of particles compared to more common approaches to PIC. This is because *Nascap-2k* uses a high order finite element potential solver. The *Nascap-2k* potential solver uses non-linear interpolating functions that guarantee strictly continuous electric fields as well as potentials. This reduces the electric field noise generated by discontinuity of electric field across grid cell boundaries.

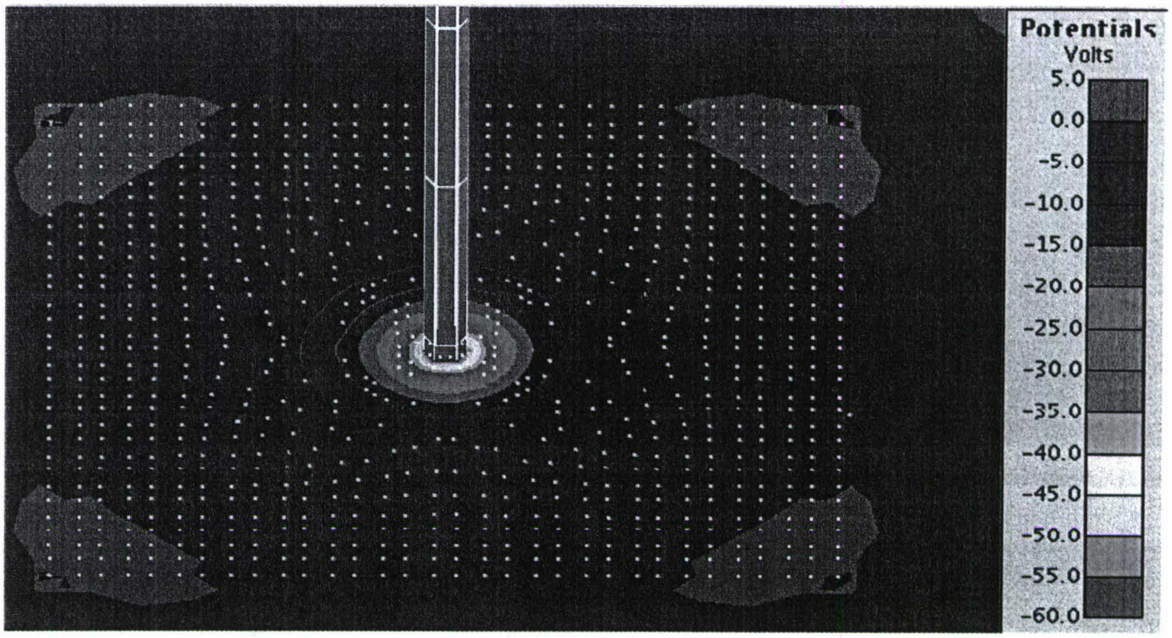

Figure 21. Subset of ion positions and potentials from 2 kHz model at time step 20 at an antenna voltage of –59 Volts.

The results are shown in Figure 22, Figure 23, and Figure 24. (Note that these figures have timesteps on the horizontal axis. The various frequencies have the same period when measured in timesteps because the simulations were all done at 50 timesteps per cycle, as indicated in **Table 2**.) With increasing frequency, the phase shift between current and voltage increases and the magnitude of current oscillation about its mean value decreases. For the 20 kHz case (Figure 24) we were able to run 6 cycles, with the latter three cycles showing a smooth, steady-state, anharmonic current waveform.

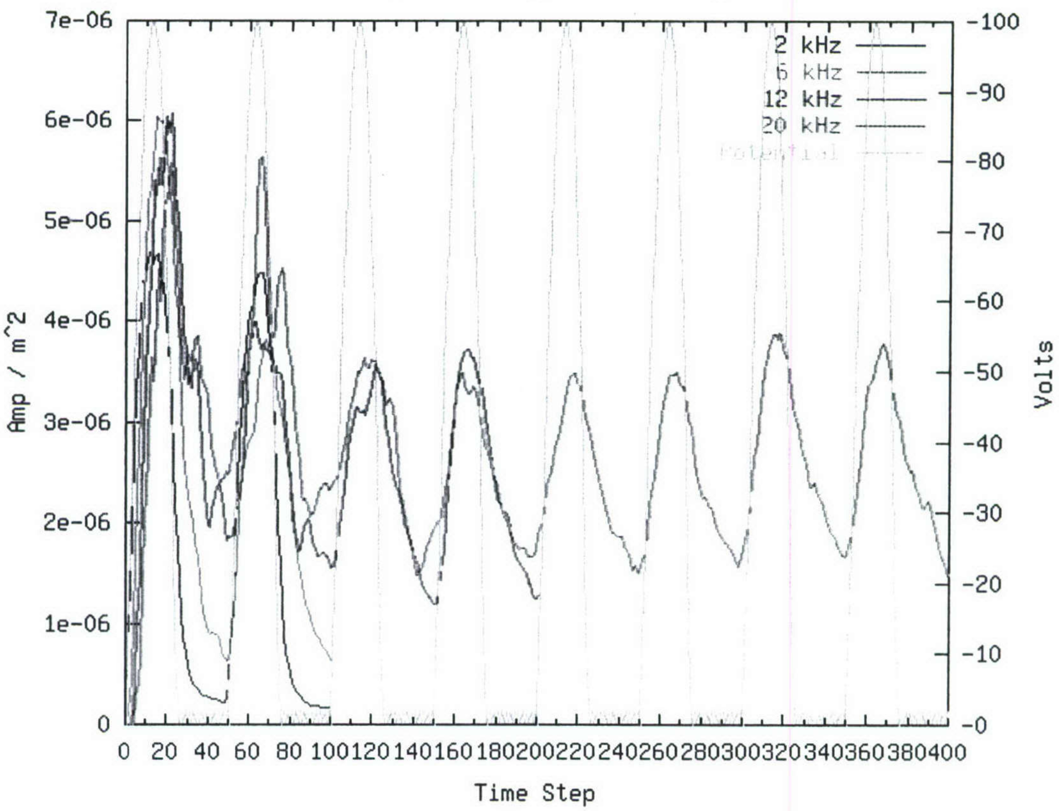

Figure 22. Current waveform results for Hybrid PIC antenna calculation in a thermal plasma at 2, 6, 12, and 20 kHz. The calculations were run at 50 timesteps per cycle, with the number of cycles increasing from two at 2 kHz to eight at 20 kHz.

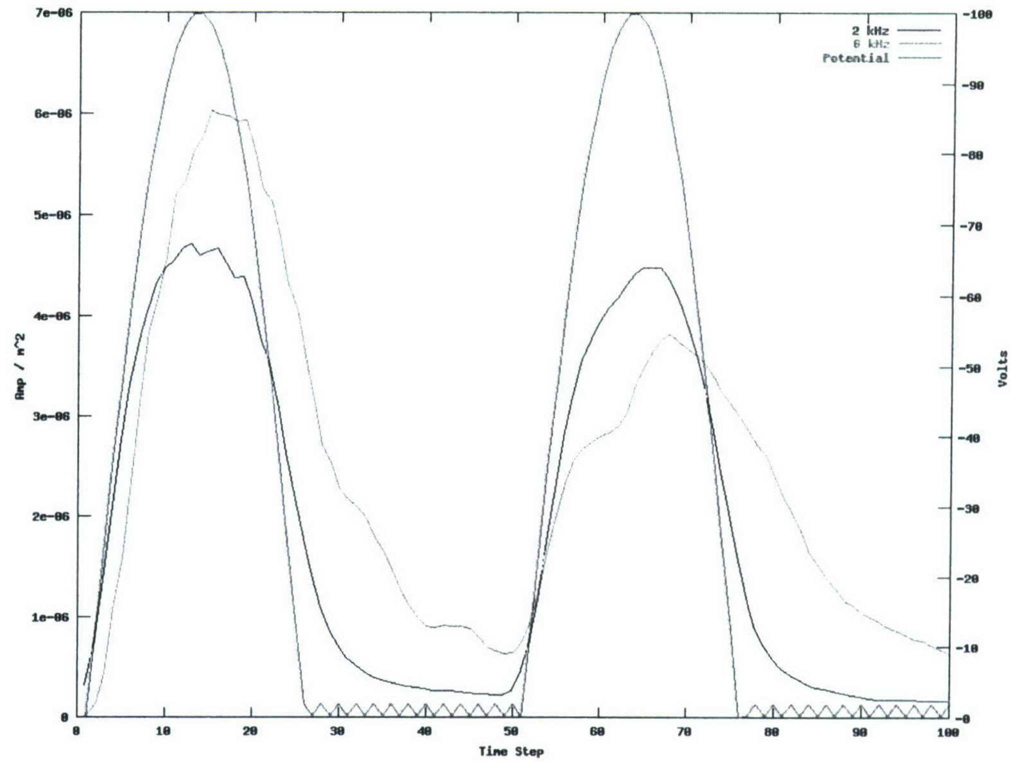

Figure 23. Current waveforms for the 2 kHz and 6 kHz cases.

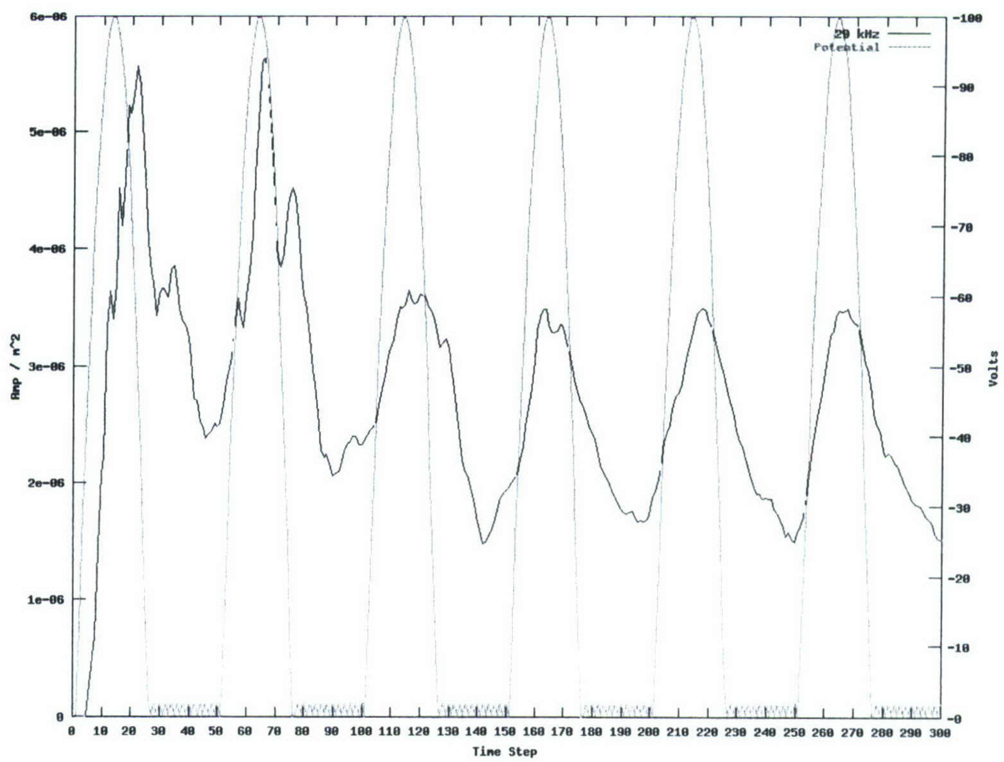

Figure 24. Current waveforms for the 20 kHz case.

Summary
We have given an overview of the *Nascap-2k* spacecraft charging and plasma interactions code, including core modeling capabilities and the methods and approaches for each type of calculation. We perform a geosynchronous charging calculation to illustrate implementation of the Boundary Element Method for calculating surface potentials and electric fields. The calculation of wake charging on the CHAWS experiment illustrates the use of iterating potentials and trajectories to a self-consistent solution. For the calculation of an electrostatic thruster plume Nascap-2k imports the plume source densities and solves a nonlinear Poisson equation for space potentials using the surface potentials as boundary conditions. Finally full-PIC calculations (dynamic ions and electrons) and hybrid-PIC calculations (dynamic ions and electrons in thermal equilibrium) are performed to model sheath structure and ion collection by a VLF antenna.

These examples illustrate the greatly improved ease of use of the code, as well as its extended capabilities. *Object Toolkit* enables users to build appropriately resolved spacecraft surface models with the needed surface attributes without needing to acquire and learn a more complex CAD program intended for some other purpose. Implementation of the BEM model allows tenuous plasma problems to be run without the need to solve potentials through all space, and also gives much more accurate surface electric fields. Issues of current interest and importance, such as Solar Wind and thruster plume environments, have been added. The code's PIC capabilities have been demonstrated, and improvements in this area are continuing. The GUI has been developed to make it easy to set up standard problems and to extend them to novel applications, as well as to facilitate the retrieval and display of graphical and numeric results.

Specifics of the physics and algorithms used in *Nascap-2k*, and comparison of results with data, can be found in proceedings of the Spacecraft Charging Technology Conferences[19,20,21,22,23,24,25,26,27,28], in the open literature[29,30,31,32], and in the *Nascap-2k* Version 3.1 User's Manual.

Acknowledgements: AFRL and the authors would like to thank NASA and the Space Environments and Effects Program, SEE, at NASA's Marshall Spaceflight Center for their significant investment in *Nascap-2k*. *Nascap-2k* is distributed by SEE at NASA/MSFC, Huntsville, Alabama, http://see.msfc.nasa.gov/.

References

[1] I. Katz, G.A. Jongeward, V.A. Davis, M.J. Mandell, R.A. Kuharski, J.R. Lilley, Jr., W.J. Raitt, D.L. Cooke, R.B. Torbert, G. Larson, and D. Rau, Structure of the Bipolar Plasma Sheath Generated by SPEAR I, *J. Geophysical Research, 94*, A2, p. 1450, 1989.

[2] M.J. Mandell, G.A. Jongeward, D.L. Cooke, W.J. Raitt, "SPEAR 3 flight analysis: Grounding by neutral gas release and magnetic field effects on current distribution," *J. Geophys. Res. 101*, A1, p. 439, 1998.

[3] Davis, V. A., M. J. Mandell, D. L. Cooke, L. Enloe, "High-Voltage Interactions in Plasma Wakes: Simulation and Flight Measurements from the Charge Hazards and Wake Studies (CHAWS) Experiment," *Journal of Geophysical Research 104*, 12445-12459, 1999.

[4] M. J. Mandell, P. R. Stannard, I. Katz, *NASCAP Programmer's Reference Manual,* NASA CR 191044, 1993.

[5] P. R. Stannard, I. Katz, L. Gedeon, J.C. Roche, A.G. Rubin, M.F. Tautz, *Validation of the NASCAP Model using Spaceflight Data*, AIAA -82-0269, 1982.

[6] I. Katz, P. R. Stannard, L. Gedeon, J.C. Roche, A.G. Rubin, M.F. Tautz, "NASCAP Simulations of Spacecraft Charging of the SCATHA Satellite," *Spacecraft/Plasma Interactions and Their Influence on Field and Particle Measurements*, ES SP-198, edited by A. Pedersen, D. Guyenne, and J. Hunt, European Space Agency, Noordwijk, The Netherlands, p. 190, 1983.

[7] M.J. Mandell and V.A. Davis, *User's Guide to NASCAP/LEO,* SCUBED report number SSS-R-85-730-R2. 1990.

[8] M.J. Mandell, and I. Katz, "High Voltage Plasma Interactions Calculations Using NASCAP/LEO," AIAA Paper AIAA-90-0725, 1990.

[9] J.R. Lilley, Jr., D.L. Cooke, G.A. Jongeward, I. Katz, *POLAR User's Manual*, GL-TR-89-0307, Oct. 1989.

[10] M.J. Mandell, T. Luu, J. Lilley, G. Jongeward, and I. Katz, *Analysis of Dynamical Plasma Interactions with High Voltage Spacecraft,* (2 volumes), Rep. PL-TR-92-2258, Phillips Lab., Hanscom Air Force Base, MA, June 1992.

[11] M.J.Mandell, I. Katz, J.M. Hilton, J. Minor, D.L. Cooke, "*Nascap-2k*, A Spacecraft Charging Analysis Code for the 21st Century," AIAA Paper 2001-0957, AIAA Aerospace Sciences Meeting & Exhibit, 39th, Reno, NV, Jan. 2001.

[12] S. A. Brebbia, *Boundary Element Methods*, Springer Verlag, New York, 1981.

[13] M.J. Mandell, G.A. Jongeward, D.L. Cooke, W.J. Raitt, "SPEAR 3 flight analysis: Grounding by neutral gas release and magnetic field effects on current distribution," *JGR*. 101, A1, p. 439, 1998.

[14] C. K. Purvis, H. B. Garrett, A. C. Whittlesey, N. J. Stevens, *Design Guidelines for Assessing and Controlling Spacecraft Charging Effects*, NASA TP 2361, 1984.

[15] Mikellides, I. G., M. J. Mandell, R. A. Kuharski, V. A. Davis, B. M. Gardner, J. Minor, "The Electric Propulsion Interactions Code," 8th Spacecraft Charging Technology Conference, Huntsville, AL, October 2003.

[16] Mandell, M. J., "NEXT Multi Ion Engine Test: Plume Modeling and Test Plans," 29th International Electric Propulsion Conference, Princeton University, 2005, paper IEPC-2005-285.

[17] Sengupta, A., *et al.*, "Status of the Extended Life Test of the Deep Space 1 Flight Spare Ion Engine after 30,352 Hours of Operation," AIAA-2003-4558, July 2003.

[18] Mandell, M. J. *et al.*, "NEXT Multiple Engine Tests: Modeling and Results," AIAA-2006-5185, 42nd AIAA/ASME/SAE/ASEE Joint Propulsion Conference, Sacramento, CA, July 2006.

[19] Mandell, M. J., I. Katz, D. Cooke, "Towards a More Robust Spacecraft Charging Algorithm," 6th Spacecraft Charging Technology Conference, Hanscom AFB, MA, 26-29 October, 1998.

[20] Katz, I., M. Mandell, B. Gardner, R. Maurer, "MESSENGER Spacecraft Charging Analysis," 7th Spacecraft Charging Technology Conference, Noordwijk, The Netherlands, April, 2001.

[21] Mandell, M. J., I. Katz, J. M. Hilton, D. L. Cooke, J. Minor, "Nascap-2K Spacecraft Charging Models: Algorithms and Applications," 7th Spacecraft Charging Technology Conference, Noordwijk, The Netherlands, April, 2001.

[22] Neergaard, L. F., J. I. Minow, M. McCollum, I. Katz, M. Mandell, V. Davis, J. Hilton, D. Cooke, "Comparision of the NASCAP/GEO, SEE Interactive Charging Handbook, and Nascap-2K Spacecraft Charging Codes," 7th Spacecraft Charging Technology Conference, Noordwijk, The Netherlands, April, 2001.

[23] Mandell, M. J., V. A. Davis, B. M. Gardner, I. G. Mikellides, D. L. Cooke, J. Minor, "Nascap-2k – An Overview," 8th Spacecraft Charging Technology Conference, Huntsville, AL, October 2003.

[24] Davis, V. A., M. J. Mandell, B. M. Gardner, I. G. Mikellides, L. F. Neergaard, D. L. Cooke, J. Minor, "Validation of Nascap-2k Spacecraft-Environment Interactions Calculations," 8th Spacecraft Charging Technology Conference, Huntsville, AL, October 2003.

[25] Mandell, M. J., D. L. Cooke, "Nascap-2k as a PIC Code," 8th Spacecraft Charging Technology Conference, Huntsville, AL, October 2003.

[26] Mandell, M. J., V. A. Davis, D. L. Cooke, A. T. Wheelock, "Nascap-2k Spacecraft Charging Code Overview," 9th Spacecraft Charging Technology Conference, Tsukuba, Japan, April 4-8, 2005.

[27] Davis, V. A., M. J. Mandell, F. J. Rich, D. L. Cooke, "Reverse Trajectory Approach to Computing Ionospheric Currents to the Special Sensor Ultraviolet Limb Imager on DMSP," 9th Spacecraft Charging Technology Conference, Tsukuba, Japan, April 4-8, 2005.

[28] Mandell, M. J., V. A. Davis, D. L. Cooke, A. T. Wheelock, C. J. Roth, "Nascap-2k Simulations of a VLF Plasma Antenna," 9th Spacecraft Charging Technology Conference, Tsukuba, Japan, April 4-8, 2005.

[29] Mandell, M. J., D. L. Cooke, V. A. Davis, G. A. Jongeward, B. M. Gardner, R. A. Hilmer, K. P. Ray, S. T. Lai, L. H. Krause, "Modeling the charging of geosynchronous and interplanetary spacecraft using Nascap-2k," Advances in Space Research 36, 2511-2515 (2005).

[30] Mandell, M., I. Katz, J. Chott, D. Cooke, "Potential Control Analysis for the C/NOFS Satellite Using NASCAP-2K", AIAA Paper 2002-0627 (2002).

[31] Mandell, M. J., I. Katz, J. M. Hilton, J. Minor and D. L. Cooke, "NASCAP2K – A Spacecraft Charging Analysis Code for the 21st Century", AIAA Paper 2001-0957 (2001).

[32] Mandell, M. J., G. Jongeward, D. L. Cooke and W. J. Raitt, "SPEAR 3 Flight Analysis: Grounding by Neutral Gas Release, and Magnetic Field Effects on Current Distribution", Journal of Geophysical Research 103, 439 (1998).